ISSN 0022-4766, Journal of Structural Chemistry, 2019, Vol. 60, No. 7, pp. 1173-1179. © Pleiades Publishing, Inc., 2019.
Text © The Author(s), 2019, published in Zhurnal Strukturnoi Khimii, 2019, Vol. 60, No. 7, pp. 1219-1225.

SYNTHESIS, CRYSTAL STRUCTURE, ANTI-BONE CANCER ACTIVITY AND MOLECULAR DOCKING INVESTIGATIONS OF THE HETEROCYCLIC COMPOUND 1-((2S,3S)-2-(BENZYLOXY)PENTAN-3-YL) -4-(4-(4-(4-HYDROXYPHENYL)PIPERAZIN-1-YL) PHENYL)-1H-1,2,4-TRIAZOL-5(4H)-ONE

G. Lv[1], D.-L. Zhang[1], D. Wang[1], L. Pan[2], and Y. Liu[2]*

Heterocyclic compound 1-((2S,3S)-2-(benzyloxy)pentan-3-yl)-4-(4-(4-(4-hydroxyphenyl)piperazin-1-yl)phenyl)-1H-1,2,4-triazol-5(4H)-one (**1**) designed using 4-(4-(4-aminophenyl)piperazin-1-yl)phenol (**2**) and (S)-N′-(2-(benzyloxy)propylidene)formohydrazide (**3**) as start materials is successfully obtained *via* a multistep synthesis and finally characterized by IR, ^{1}H NMR, and single crystal X-ray diffraction. In addition, the *in vitro* anticancer activities of newly synthesized compound **1** are evaluated against three human bone cancer cell lines U2OS, Saos-2, and GC9811. In addition, the molecular docking is used to study the potential antiviral activity of **1** by calculating the binding sites for the 1AS0 protein.

DOI: 10.1134/S0022476619070205

Keywords: heterocycles, X-ray crystallography, anticancer activity.

INTRODUCTION

Posaconazole is an antifungal agent used against a wide range of fungal pathogens, including both yeast and molds [1-3]. As one of the most important intermediates in the synthesis of Posaconazole, 1-((2S,3S)-2-(benzyloxy)pentan-3-yl)-4-(4-(4-(4-hydroxyphenyl)piperazin-1-yl)phenyl)-1H-1,2,4-triazol-5(4H)-one (**1**) has been less studied on its bioactivity properties compared with widely explored Posaconazole [4-6]. Recent publications have revealed that some compounds with 1,2,4-triazol moieties are perspective scaffolds for the design of anticancer drugs [7, 8]. Thus, our attention has been drawn to the synthesis, characterization, and crystal structure of compound **1** with substituted 1,2,4-triazol groups whose anticancer activity has never been reported before.

The present work deals with the synthesis and characterization of title compound **1**. Compound **1** was synthesized using 4-(4-(4-aminophenyl)piperazin-1-yl)phenol (**2**) and (S)-N′-(2-(benzyloxy)propylidene) formohydrazide (**3**) as start materials producing 5-bromo-2-methylbenzoyl chloridephenyl (4-(4-(4-hydroxyphenyl)piperazin-1-yl)phenyl)carbamate (**4**)

[1]Inner Mongolia University For The Nationalities, Tongliao, Inner Mongolia Autonomous Region, P. R. China; *liuyang0919@126.com. [2]First Affiliated Hospital of Inner Mongolia University For The Nationalities, Tongliao, Inner Mongolia Autonomous Region, P. R. China. Original article submitted December 4, 2018; revised February 14, 2019; accepted February 18, 2019.

and N′-((2S,3S)-2-(benzyloxy)pentan-3-yl)formohydrazide (**5**) respectively, and title compound **1** was prepared after the reaction of compounds **4** and **5** (Scheme 1). In addition, the *in vitro* anticancer activity of compound **1** on three human bone cancer cells (U2OS, Saos-2, and GC9811) was further determined. Finally, molecular docking studies were performed to further clarify its structure–activity relationship.

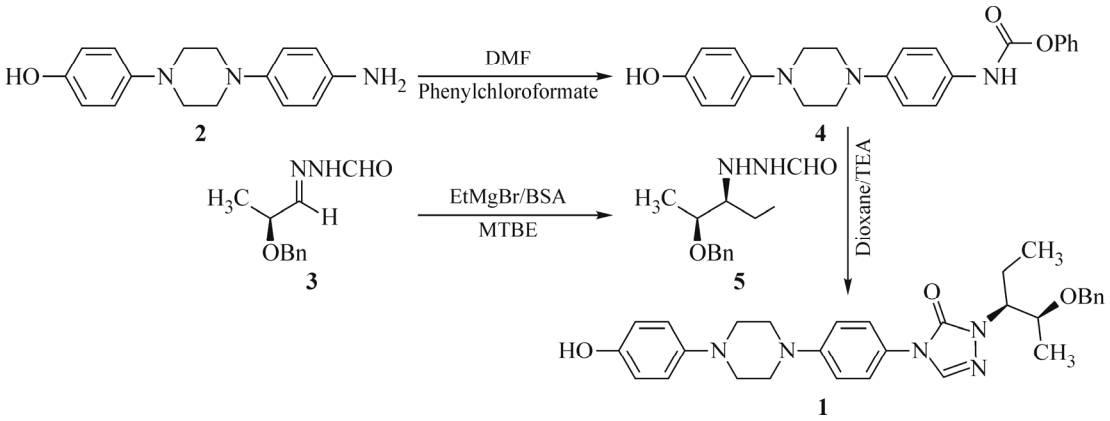

Scheme 1. The synthesis route of compound **1**.

EXPERIMENTAL

Apparatus and materials. IR spectra (400-4000 cm^{-1}) were obtained using a Brucker Equinox-55 spectrophotometer. ^1H NMR spectra were obtained using a Varian Inova-400 spectrometer (at 400 MHz). Mass spectra were obtained using a microTOF-Q II mass spectrometer. The melting points were taken on a XT-4 micro melting apparatus, and the thermometer was uncorrected.

Synthesis and characterization of compounds 4, 5, and 1. Phenyl chloroformate (13.95 g, 0.089 mol) was added to a pre-cooled solution of compound **2** (20 g, 0.074 mol) in dimethylformamide (140 mL) at 0-10 °C. After the completion of the reaction, the reaction mixture was quenched with water. Ispropyl alcohol (IPA, 60 mL) was added to the solid and the mixture was heated to 60-65 °C and stirred for 1 h at the same temperature. Compound **4** was filtered off, washed with IPA, and dried. ^1H NMR (DMSO-d_6, 400 MHz): δ 3.155 (t, 8H, piperazine-CH_2), 6.685 (d, 2H, p-aminophenol-3-CH), 6.859 (d, 2H, p-aminophenol-2-CH), 6.981 (d, 2H, aniline-3-CH), 7.237 (m, 2H, aniline-2-CH), 7.406 (t, 2H, phenol-CH), 7.447 (d, 2H, phenol-CH), 8.871 (s, 1H, p-aminophenol-OH), 9.989 (s, 1H, CO_2NH). IR (KBr, λ, cm^{-1}) 3460 (s), 3368 (m), 1662 (s), 1568 (s), 1340 (s), 1160(s).

A mixture of methyl tertiary butyl ether (100 mL), Mg powder (128 g), and I_2 (0.02 g) was heated to 40-45 °C under the nitrogen atmosphere, and ethyl bromide (54.8 g) was added slowly to the reaction mixture for about 1 h. The reaction mixture was further heated to 50-55 °C, and methyl tertiary butyl ether (40 mL) was added to it. N,O-bistrimethyl silyl acetamide (BSA, 40.6 g, 0.2 mol) was added to a mixture of methyl tertiary butyl ether (100 mL) and compound **3** (20 g, 0.097 mol) over a period of 45 min and stirred at 25-30 °C for 1 h. Compound **5** was obtained by concentrating under vacuo and taken into the next step without isolating. ^1H NMR (DMSO-d_6, 400 MHz): δ 0.865 (t, 3H, CH_3), 0.927 (m, 2H, CH_2), 1.129 (d, 3H, CH_3), 2.503 (m, 1H, N–CH), 3.581 (m, 1H, O–CH), 4.408 (m, 2H, Ar–CH_2), 7.307 (m, 5H, Ar–H), 8.26 (s, 1H, CO–H). IR (KBr, λ, cm^{-1}) 3431 (br), 3236 (m), 3083 (m), 2566 (m), 1717 (s), 1672 (m), 1587 (s), 1302 (s), 1163 (s).

A mixture of compounds **4** (18.0 g, 0.046 mol), **5** (16.38 g, 0.069 mol), and dioxane (180 mL) was heated to 90-100 °C. Triethylamine (9.36 g, 0.092 mol) was added to the reaction mixture and then stirred for 24 h at 90-100 °C. After the completion of the reaction, the reaction mixture was cooled to 25-30 °C and dichloromethane (25 mL) was added to the reaction mixture. Compound **1** was obtained by filtration and concentration under vacuo and stirred in isopropyl alcohol (27 mL) at 25-30 °C for 6 h. Pure compound **1** was got by recrystallization with methanol. ^1H NMR (DMSO-d_6, 400 MHz):

δ 0.793 (t, 3H, CH_3), 1.242 (d, 3H, CH_3), 1.765 (q, 2H, CH_2), 3.122 (t, 4H, piperazine-CH_2), 3.327 (t, 4H, piperazine-CH_2), 3.745 (m, 1H, N–CH), 3.990 (m, 1H, O–CH), 4.275-4.544 (d, 2H, Ar–CH_2), 6.691 (d, 2H, Ar–H), 6.869 (d, 2H, Ar–H), 7.119 (d, 2H, Ar–H), 7.172 (q, 2H, Ar–H), 7.232 (m, 3H, Ar–H), 7.476 (d, 2H, Ar–H), 8.323 (s, 1H, N_2C–H), 8.787 (s, 1H, Ar–OH). HRMS (ESI^+): *m*/*z*: calcd for $C_{30}H_{35}N_5O_3$: 536.2638 [$M+Na^+$]; found: 536.2619. IR (KBr, λ, cm^{-1}): 3468.1 (s), 1678.2 (s), 1605.1 (m), 1485.07 (s), 1231.9 (s), 1115.4 (s).

Crystal structure determination. A suitable single crystal of compound **1** (obtained by slow volatilization of its CH_2Cl_2 solution) was carefully selected under an optical microscope and glued on thin glass fibers. The intensity data on **1** was collected on an Oxford Xcalibur E diffractometer. The empirical absorption corrections were applied to the data using the SADABS system. This structure was solved by a direct method and refined by the full-matrix least-squares method on F^2 using the SHELXS-97 program [9]. All non-hydrogen atoms of **1** were refined anisotropically, and all the hydrogen atoms attached to carbon atoms were fixed at their ideal positions. Pertinent crystal data and structural refinement results for compound **1** were summarized in Table 1.

Anticancer activity. The anticancer activity of compound **1** against three human bone cancer cells (U2OS, Saos-2, and GC9811) was determined using the MTT [3-(4,5-dimethyl-2-thiazolyl)-2,5-diphenyl-2-H-tetrazolium bromide] assay [10]. In this study, the cells were plated on 96-wells at 5×10^3. After the attachment (24 h), the cells reaching 70-80% confluency were treated for 48 h with each compound at different concentrations or 1% dimethyl sulfoxide (DMSO) as a negative control. After 48 h incubation, 20 μL of the MTT solution (5 mg/mL in phosphate buffer saline (PBS)) was added and incubated for additional 4 h. Subsequently, the medium was aspirated carefully, and 150 μL of DMSO was added. After incubation for 15 min, the optical density was measured at 490 nm using a FlexStation 3 benchtop multi-mode microplate reader (Molecular Devices, USA). This assay measures the amount of formazan produced from MTT by dehydrogenase enzymes of metabolically active cells. Thus, the quantity of formazan produced is directly proportional to the number of living cells. Absorbance values of the treated cells were compared with the absorbance values of untreated cells. The IC_{50} and IC_{90} values were determined from the nonlinear regression equation. The results are presented as the average percentage viability to the negative control (1% DMSO).

TABLE 1. Crystal Data and Structure Refinements for Compound **1**

Formula	$C_{30}H_{35}N_5O_3$
M_r	513.63
Crystal system	Monoclinic
Space group	$P\,2_1$
a, *b*, *c*, Å	7.8248(2), 8.1160(2), 21.8897(5)
β, deg.	100.202(2)
V, $Å^3$	1368.15(6)
Z	2
Crystal size, mm	0.49×0.4×0.23
D_{calc}, g/cm^3	1.247
μ(CuK_α), mm^{-1}	0.657
θ range, deg.	2.051-66.932
Reflections collected	23158
No. unique data [*R*(int)]	4809 [0.0416]
No. data with $I \geq 2\sigma(I)$	4493
R_1	0.0370
ωR_2 (all data)	0.0969
CCDC	1867276

Simulation details. The structure of compound **1** was optimized by density functional theory (DFT) using a B3LYP/6-31G(*d*) basis set. The structure optimization and energy calculations were performed with the GAUSSIAN 09 program.

AutoDock Vina v1.2 has been utilized to study the binding mode of compound **1** with tubulin [11]. Tubulin was used as downloaded without a further modification from the protein data bank (PDB ID: 1AS0). The geometry structures of compounds A and B were optimized through quantum chemistry calculations by Gaussian 09 at the B3LYP theory of level with the 6-31G* basic set. AutoDockTools v1.5.6 has been adopted to transfer 1AS0 and optimized structures A and B to AutoDock Vina input files. Only polar hydrogen atoms on these structures are considered. The center coordinates of the search grid of tubulin were set to 38.15, –26.99 and 6.18, respectively; the length of the search grid was 15. All parameters needed for AutoDock Vina are used as default if not mentioned specifically. The calculated results were analyzed and visualized by PyMoL v1.8.6.

RESULTS AND DISCUSSION

Molecular structure. The crystal structure of compound **1** ($C_{30}H_{35}N_5O_3$) was obtained by the single crystal X-ray diffraction analysis. The result indicates that the compound belongs to the triclinic crystal system with the space group $P2_1$. The target compound shows a two-dimensional layered structure with two kinds of hydrogen bonds: C–H···O and O–H···O. The molecular structural unit of **1** is shown in Fig. 1. In the structural unit, the dihedral angle of the five-membered ring containing two nitrogen atoms (C(13), C(14), N(1), N(2), and N(3)) and the adjacent six-membered carbon ring (C(15)–C(20)) is 70.79°. The C–C, C–N, and C–O bond distances are in the ranges 1.351(7)-1.530(4) Å, 1.361(3)-1.455(3) Å, and 1.222(3)-1.423(3) Å, respectively. All of these bond lengths are in their normal ranges and are comparable with those of the previously examined structures.

Furthermore, the two kinds of hydrogen bonds (C–H…O and O–H…O) could be found in the packing structure of **1**. The detailed information on the hydrogen bonding is provided in Table 2. By means of two types of interactions of hydrogen bonds, a two-dimensional layered structure is generated. Fig. 2 shows its crystal packing structure along the *a* axis. These hydrogen bonds play a significant role in its structural stability.

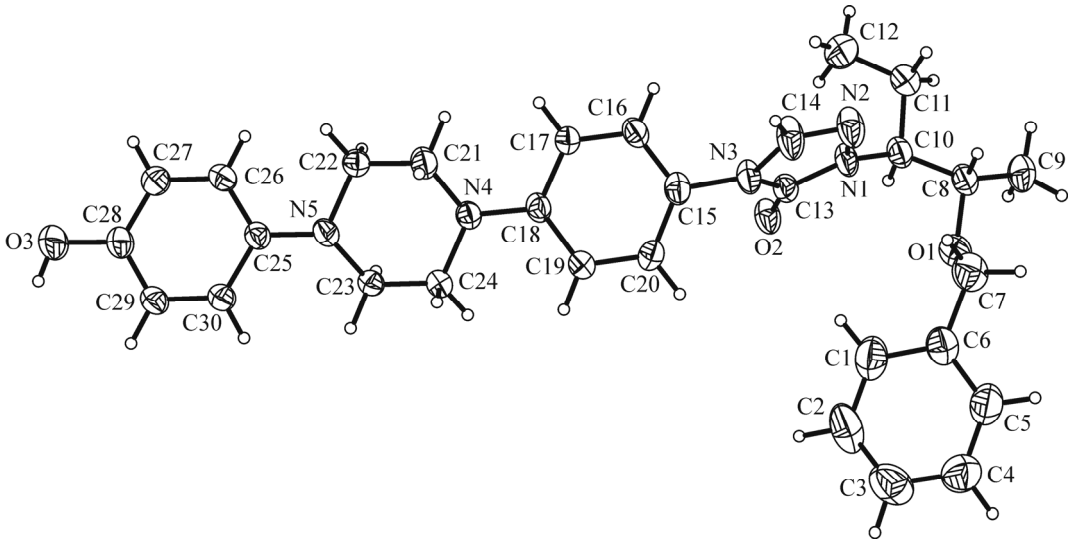

Fig. 1. The molecular structural unit for compound **1**.

TABLE 2. Hydrogen Bonds in Compound **1**

D–H…A	D–H, Å	H…A, Å	D…A, Å	D–H…A, deg.	Symmetry code
O3–H3…O2	0.82	2.04	2.816(3)	158	2–*x*, –1/2+*y*, 1–*z*
C2–H2…O3	0.93	2.51	3.286(5)	141	2–*x*, –1/2+*y*, 1–*z*

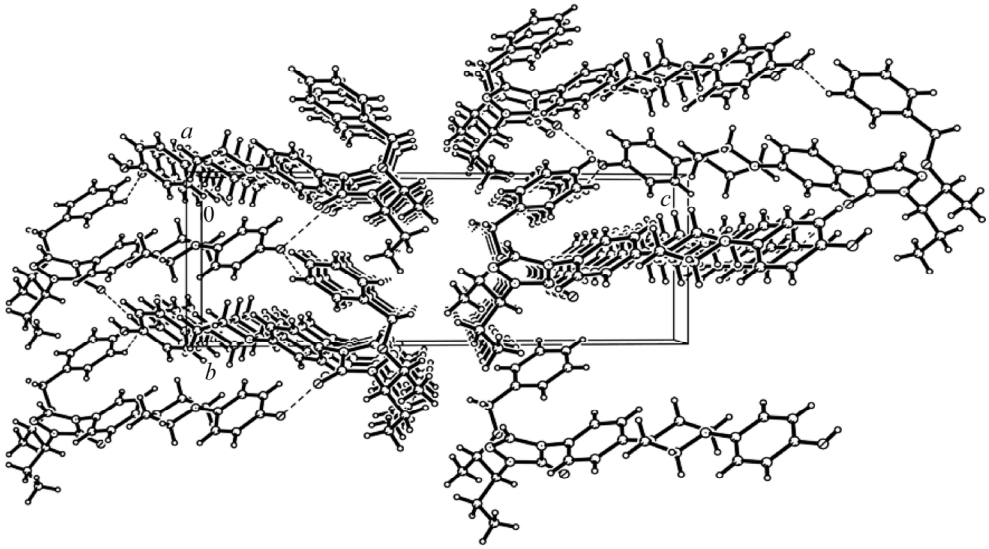

Fig. 2. View of the crystal packing structure of compound **1** along the *a* axis.

Anticancer activity. The interesting structural features of **1** encouraged us to test its cytotoxicity against three human bone cancer cell lines (U2OS, Saos-2, and GC9811) along with normal mouse embryonic fibroblast (NIH 3T3) cells by the MTT assay method. Compounds were dissolved in DMSO and blank samples containing the same volume of DMSO were taken as controls to identify the activity of the solvent in this cytotoxicity experiment. Cisplatin was used as a positive control to assess the cytotoxicity of the test compounds. The results were analyzed by means of cell inhibition expressed as IC_{50} values and are shown in Table 3. The IC_{50} values of compound **1** showed that it exhibited a significant activity against U2OS, Saos-2, and GC9811 cell lines, which was almost equal to the activity of the well-known anticancer drug, cisplatin. The results of the *in vitro* cytotoxic activity studies have also indicated that the IC_{50} value of **1** against NIH 3T3 (normal cells) was above 350 μM, which confirmed that the compound is very specific for cancer cells and even less toxic compared to cisplatin (IC_{50} = 198 μM).

Molecular docking. In order to perform the molecular docking calculation, the precise structure of compound **1** is optimized by DFT calculations. Considering only the structure was needed, we chose the widely used B3LYP/6-31G(*d*) method to implement the geometry optimization. The initial structure for the geometry optimization is taken from the experimental measurement (Fig. 3). Several selected parameters for both experiment and simulation are summarized in Table 4; the maximum absolute deviations for bonds, bond and dihedral angles are 0.02 nm, 1.7° and 27.4°, respectively. Such deviations can be easily explained since the geometry optimization is performed in the gas phase without any constrains

TABLE 3. Cytotoxic Activity of Compound **1** and Cisplatin

Compounds	Half maximum inhibitory concentration in μM (IC_{50})			
	U2OS	Saos-2	GC9811	NIH 3T3
1	13.1±1.9	11.7±2.1	14.6±2.7	359±7
Cisplatin	12.5±0.7	13.8±0.8	10.5±1.8	198±11

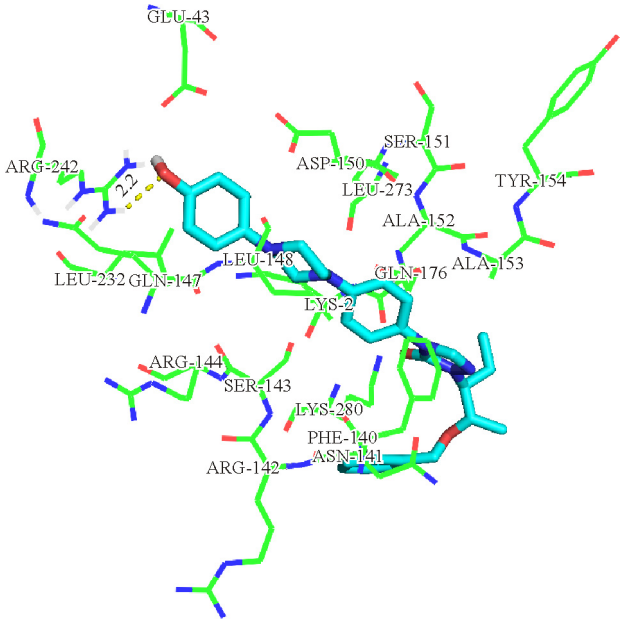

Fig. 3. The most favorable binding mode between compound **1** (stick) and the neighboring residues from protein 1AS0; the labels of the residues, the hydrogen bond as well as its length are shown explicitly.

TABLE 4. Experimental and Calculated Structural Parameters of the Selected Bond Lengths, Bond Angles and Torsions of Compound **1**

Parameter	X-ray	Calculation
	Bond length, Å	
O3–C28	1.369	1.371
N5–C25	1.418	1.422
N4–C18	1.401	1.411
N3–C15	1.438	1.421
N1–C10	1.455	1.459
O1–C8	1.423	1.426
	Angle / Torsions, deg.	
C13–N3–C15	125.5	125.9
N2–N1–C10	120.1	120.9
C9–C8–O1	108.5	110.2
O2–C13–N3–C15	–9.5	–3.2
N2–N1–C10–C11	–65.9	–57.9
C7–O1–C8–C9	114.6	87.2

while in the experiment, the molecules in the crystal are influenced by the neighboring molecules, However, excellent agreement has been achieved between the experiment and the simulation.

The global minimum structure of compound **1** is used to perform the autodocking simulation. The binding pocket is provided by protein 1AS0, which is quite general for the investigation of the antivirus capability of chemical structures. Since compound **1** is a large molecule, only 5 possible binding modes are found and the most preferable binding mode is shown in Fig. 3. We can see that the long arm has been inserted into the binding pocket; the polar interaction is formed between the carbonyl oxygen atom at the end of the arm and a hydrogen atom on residue ARG-242. The other heteroatoms either on the

middle ring of the arm or on the rest of the moieties do not contribute any interactions with surrounding residues, such as ASP-150, LEU-273, LEU-148, SER-143, and ALA-152. The corresponding binding energy and the length of the polar interaction are –4.5 kcal/mol and 2.2 Å, which shows good potential of the antivirus capability.

CONCLUSIONS

In conclusion, we have successfully synthesized heterocyclic compound 1-((2S,3S)-2-(benzyloxy)pentan-3-yl)-4-(4-(4-(4-hydroxyphenyl)piperazin-1-yl)(phenyl)-1H-1,2,4-triazol-5(4H)-one (**1**) and characterized it *via* IR, ^{1}H NMR, HRMS, and single crystal X-ray diffraction. The MTT assay shows that compound **1** may act as a novel anticancer drug in the future for its *in vitro* anticancer activities against three human bone cancer lines U2OS, Saos-2, and GC9811, which is further supported via the molecular docking simulations.

FUNDING

This work was supported by grants from the Natural Science Foundation of Inner Mongolia University For The Nationalities (NMDYB1723).

CONFLICT OF INTERESTS

The authors declare that they have no conflict of interests.

REFERENCES

1. F. B. Sime, J. Stuart, J. Butler, T. Starr, S. C. Wallis, S. Pandey, J. Lipman, and J. A. Roberts. *Int*. *J*. *Antimicrob*. *Agents*., **2018**, *52*, 506.
2. D. J. Greenblatt, J. S. Harmatz, M. J. Ryan, and C. R. Chow. *J. Clin. Psychopharmacol*., **2018**, *38*, 289.
3. J. M. Kozuch, A. Feist, G. Yung, L. Awdishu, S. Hays, J. P. Singer, and R. Florez. *Clin*. *Transplant*., **2018**, *32*, e13300.
4. M. T. Rosanova, C. Voto, M. S. Mussini, C. Sarkis, S. Gómez, N. Sberna, S. Carnovale, B. Caracciolo, and R. Lede. *Arch*. *Argent. Pediatr*.. **2018**, *116*, e451.
5. C. R. Chow, J. S. Harmatz, M. J. Ryan, and D. J. Greenblatt. *J. Clin. Pharmacol*., **2018**, *58*, 1436.
6. D. J. Epstein, S. K. Seo, Y. T. Huang, J. H. Park, V. M. Klimek, E. Berman, M. S. Tallman, M. G. Frattini, and G. A. Papanicolaou. *J*. *Infect*., **2018**, *77*, 227.
7. R. Lesyk, O. Vladzimirska, S. Holota, L. Zaprutko, and A. Gzella. *Eur*. *J. Med. Chem*.**, 2007**, *42*, 641.
8. E. Pomarnacka and I. Kozlarska-Kedra. *Farmaco*, **2003**, *58*, 423.
9. G. M. Sheldrick. SHELXL-97, Program for Solution Crystal Structure and Refinement. University of Göttingen, Germany, **1997**.
10. L. Kupcsik. *Methods Mol*. *Biol*., **2011**, *740*, 13.
11. O. Trott and A. J. Olson. *J. Comput*. *Chem.*, **2010**, *31*, 455.